Mater. Res. Soc. Symp. Proc. Vol. 1125 © 2009 Materials Research Society 1125-R07-04

Effects of hydrogen permeation on W, Mo and Cu Langmuir probes at ISTTOK

D. Nunes[1,3], P.A. Carvalho[1,3], R. Mateus[1], I.D. Nogueira[3], A. Moita de Deus[3], J.B. Correia[2], N. Shohoji[2], R.B. Gomes[1], H. Fernandes[1], C. Silva[1], N. Franco[4], E. Alves[4]

[1]Euratom/IST, Instituto de Plasmas e Fusão Nuclear, Instituto Superior Técnico,
Av. Rovisco Pais, 1049-001 Lisboa, Portugal
[2] LNEG, Departamento de Materiais e Tecnologias de Produção,
Estrada do Paço do Lumiar, 1649-038 Lisboa, Portugal
[3]ICEMS, Departamento de Engenharia de Materiais, Instituto Superior Técnico,
Av. Rovisco Pais, 1049-001 Lisboa, Portugal
[4]ITN, Instituto Tecnológico e Nuclear, Estrada Nacional 10, 2686-953 Sacavém, Portugal

ABSTRACT

The microstructures of tungsten, molybdenum and copper wires used as Langmuir probes at ISTTOK edge plasma have been investigated. The probes cross-sections evidenced extensive grain growth, intergranular bubbles and increased hardness at the plasma exposed regions. Internal surfaces of large bubbles exhibited slip bands resulting from plastic deformation induced by high H_2 pressure. Elastic recoil detection analysis was used to measure H concentration profiles. The present results suggest that H_2 bubble formation in first wall components under long-term high thermal loads should be closely monitored in nuclear fusion devices. Strategies for H damage mitigation are proposed and discussed.

INTRODUCTION

Both reliability and long lifetime are essential requirements for materials of first wall components. Tungsten presents great potential to fulfill these requirements due to its high melting point, high threshold for sputtering and good heat load capability [1]. These characteristics combined with low neutron activation and low tritium inventory render tungsten as potentially suitable for high flux components and high-power density structural applications in fusion reactors. Molybdenum, a similar refractory metal, is also considered a potential plasma facing material [2]. Copper alloys, on the other hand, have been chosen as heat-sink materials for ITER first wall panels due to their favorable thermal conductivity, mechanical strength and radiation resistance [3]. However, a comprehensive understanding of the damage caused by H plasmas to these materials is still required.

Energetic hydrogen ions are able to penetrate the surface barrier of metals and this ion driven permeation process can exceed gas driven permeation by several orders of magnitude. The solubility of hydrogen isotopes in tungsten, molybdenum and copper is low and hydrogen atoms are likely to come out of solution at traps such as vacancies, voids and grain boundaries, where they achieve a lower potential energy than that attained among crystalline sites [4]. The traps eventually become saturated and, even for the low gas pressure in the fusion chamber, untrapped hydrogen atoms diffuse out of the implant zone deeper into the material. At saturated traps, molecular recombination tends to occur resulting in bubbles and blisters with increasing

internal pressure. At enhanced diffusivity conditions the system can reduce the interfacial free energy by bubble and blister coarsening.

Evidence of internal bubble formation has been previously reported for W and Cu Langmuir probes exposed to H plasma [5]. In the present work, the microstructure of W and Cu probes enduringly exposed in a tokamak to low energy proton irradiation has been further investigated for long term hydrogen migration behavior. Intergranular bubble formation in a Mo probe has also been scrutinized. Hydrogen content was evaluated by elastic recoil detection analysis (ERDA) while Rutherford backscattering spectrometry (RBS) was used for normalization purposes.

EXPERIMENTAL DETAILS

Commercially pure W (99.95 wt. %, ϕ = 0.75 mm), Mo (99.95 wt. %, ϕ = 0.75 mm) and Cu (99.99 wt. %, ϕ = 2 mm) wires have been exposed at the ISTTOK tokamak edge plasma for ~200 discharges of 30 ms with intervals of 10 min. The W and Mo wires were oriented radially with an exposure length of 3 mm while the Cu wire was oriented vertically with an exposure length of 20 mm. The wire position was varied from discharge to discharge across the ISTTOK edge plasma (up to 2 cm inside the limiter position). The H_2 discharge pressure was 10^{-4} torr and the plasma parameters were: electron and ion temperatures, $T_e \sim T_i$ = 15 - 50 eV, density, n = 0.5 - 2.10^{18} m^{-3}, hydrogen flux, Γ^{H+} = 1-7×10^{22} $m^{-2}s^{-1}$ and fluence lower than 4.10^{23} particles/m^2. A total of 0.5 to 4 h of cleaning discharges was applied during the probes lifetime with $T_e \sim T_i$ = 5-10 eV, n = 1 - 5.10^{17} m^{-3} and the same H_2 discharge pressure. The shelf life of the W, Cu and Mo probes was, respectively, 4 years, 2 years and 2 months at the time of the post-mortem analysis.

Longitudinal sections of the W, Mo and Cu wires were investigated up to, respectively, 14.7 mm, 6 mm and 8.4 mm from the probe edge. Microstructural observations were carried out by scanning electron microscopy (SEM) after standard metallographic preparation. Grain size ($\sqrt{A}$) was determined from the average grain area (A) using the Jeffries planimetric method. Electron Backscatter Diffraction (EBSD) was used to refine Cu grain size. Image orientation maps were acquired at 20 kV with a 70º sample tilt, 160 x magnification and a step size of 0.6 μm using a JEOL7001 field-emission gun SEM fitted with a NordlysS EBSD detector.

The H content in W and Mo Langmuir probes was evaluated by simultaneous ERDA and RBS experiments, using a 0.3x0.3 mm^2 collimated 2.0 MeV $^4He^+$ beam. Unexposed wires of the same batches were used as reference samples. ERDA measurements were performed with a surface tilt angle of 78º and the recoiled H^+ ions were detected by a surface barrier detector placed at a scattering angle of 24º in IBM geometry. Scattered $^4He^+$ ions were retained by a mylar foil with a thickness of 8 μm located in front of the detector. RBS spectra, collected by two surface barrier detectors placed at 180 and 160º scattering angles in Cornell geometry, were used to normalize the H^+ ERDA yields. Spectra pertaining to the same sample were simultaneously analyzed and a unique solution extracted with the NDF code [6]. The cylindrical shape of the samples introduced difficulties on the quantitative analysis of the H content and only qualitative results are presented.

Hardness variations were assessed through force-displacements plots obtained with a calibrated Shimadzu DUH-W211S ultramicrohardness tester, using a Berkovich indenter, a load of 1N and a hold time at peak load of 20 s.

RESULTS AND DISCUSSION

After plasma exposure the probes exhibited shape modifications that indicate strong softening, incipient melting and/or evaporation. Similar behavior has been reported for castellated structures tested in present-day tokamaks [7,8]. The probe microstructures (figure 1) evidenced extensive grain growth and bubble nucleation at internal grain boundaries. This demonstrates that, in spite of the low fluence and irradiation energy, the H^+ ions were able to migrate inwards. Furthermore, grain boundaries acted initially as traps and subsequently as molecular recombination sinks [9]. A higher density of intergranular bubbles was present at moderately exposed regions (figure 1 (b)), while fewer but large bubbles were found at severely exposed regions (figure 1 (a)). The bubble number and size distribution suggest that large bubbles result from a coarsening process [10] closely associated with grain growth, and therefore strongly dependent on the temperature. The probes were used for diagnostic purposes at ISTTOK where they have been exposed both to plasma working cycles and long cleaning discharges. Since during the diagnostic experiments the temperature was registered in just a fraction of the effective working cycles, a complete temperature history is not available. The probes microstructure is not expected to significantly affect the low diagnostic currents measured. However, the observed behavior may condition the lifetime of first wall components under high thermal loads in larger fusion devices.

H_2 bubbles at W grain boundaries [11] and T_2 bubbles at Cu grain boundaries [12] have been previously reported. The ability of absorbing H is common to all metals [13] which are therefore susceptible to hydrogen damage [14]. Hydrogen damage by blistering or bubble nucleation occurs when H atoms continuously reach the traps, where molecular recombination takes place inducing pressure build up and host atom ejection from lattice sites. The bubble formation process is therefore critically dependent on the temperature through H diffusion rate and thermal vacancy concentration. The process is assisted by plastic deformation as evidenced by the presence of slip bands on the internal surface of large bubbles (figure 2). Equilibrium H_2 gas pressures can be very high even for small H concentrations in the lattice [13] and must be comparable to the metal yield strength (at the service temperature) to induce plastic deformation [15]. Slip bands are also common in fracture surfaces associated with hydrogen embrittlement [16]. Hydrogen has been proposed to favor the localization of deformation associated with slip bands through the hydrogen enhanced localized plasticity (HELP) mechanism [17]. In this mechanism H diffuses through interstitial lattice sites toward regions of lower chemical potential, such as dislocation cores where it forms Cottrell atmospheres. These atmospheres shield the stress fields of adjacent dislocations of same signal, favoring the formation of slip bands at free surfaces.

Figure 3 presents the ERDA results of W and Mo probes. The H content of the plasma exposed Mo probe was higher both at the superficial and deeper layers than in the unexposed material. In spite of the long shelf life of the W probe, the analysis showed a strong superficial H presence and a higher concentration in deeper layers when compared with unexposed material. These results point to significant long term H retention in the exposed materials. The low release rate is probably related to high bond energy traps and recombined H_2 in bubbles.

Figure 4 presents the experimental relation between hardness and grain size for the W and Cu probes (in the case of Cu, grain size determination was refined by EBSD to take twins into account). Literature Hall-Petch relations [18-20] are also shown (straight lines). The results demonstrate a significant increase of strength which can be justified by tH presence. In fact, although Cottrell atmospheres tend to favor localized plasticity, they stabilize edge character dislocations and therefore restrict cross-slip. Furthermore, dissolved H is a moderate solution hardener [16,21] and small bubble dispersions contribute to hardening by an Orowan mechanism [15].

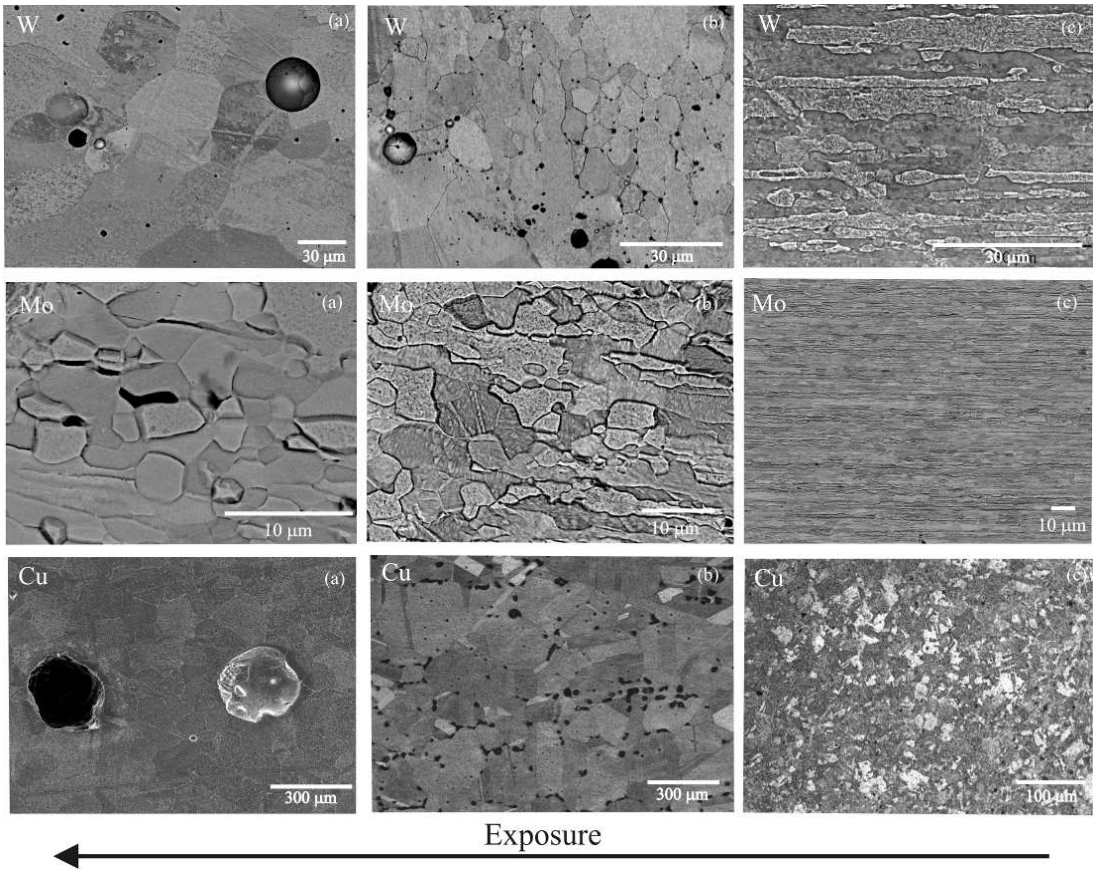

Figure 1. Probe microstructure: (a) severely exposed, (b) moderately exposed and (c) unexposed.

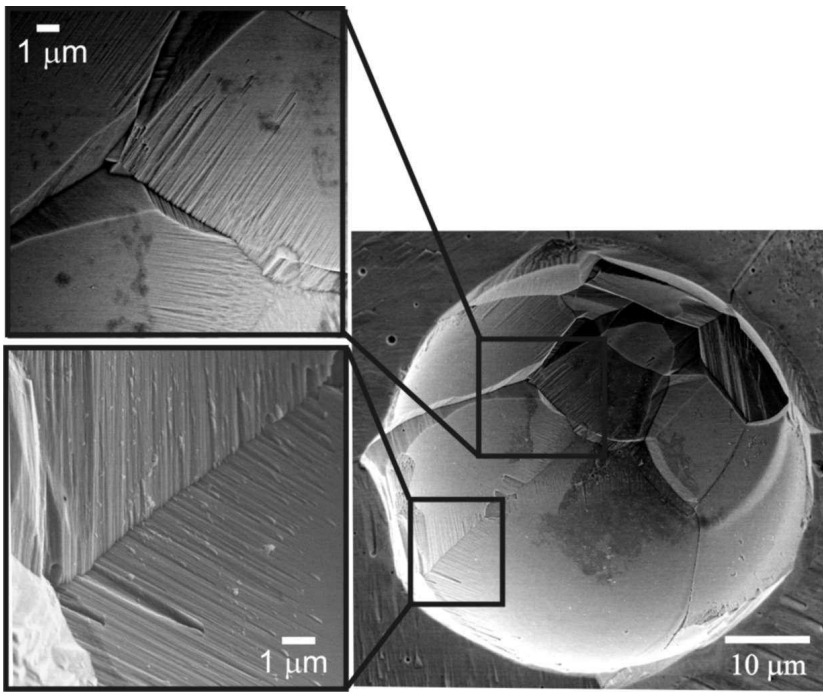

Figure 2. Large bubble in W evidencing slip bands at the internal surface.

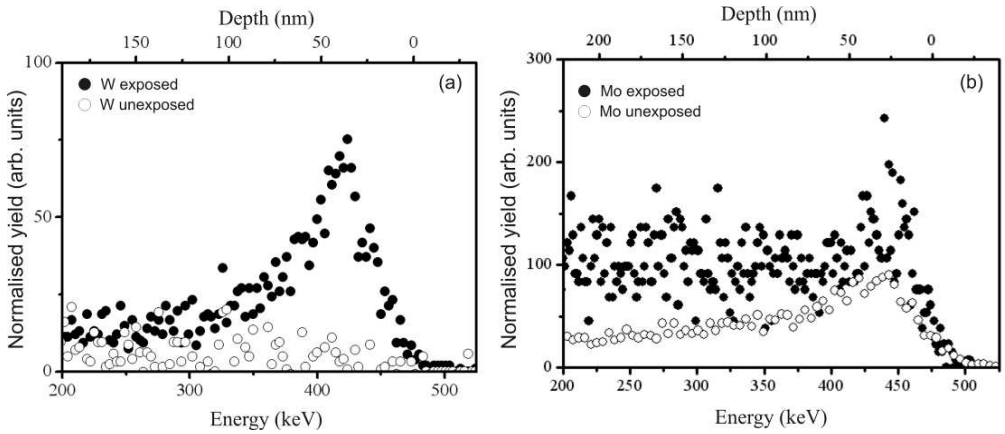

Figure 3. ERDA yields of plasma exposed (dark circles) and unexposed (open circles) (a) W and (b) Mo. Depth scales were calculated considering the existence of pure W and Mo.

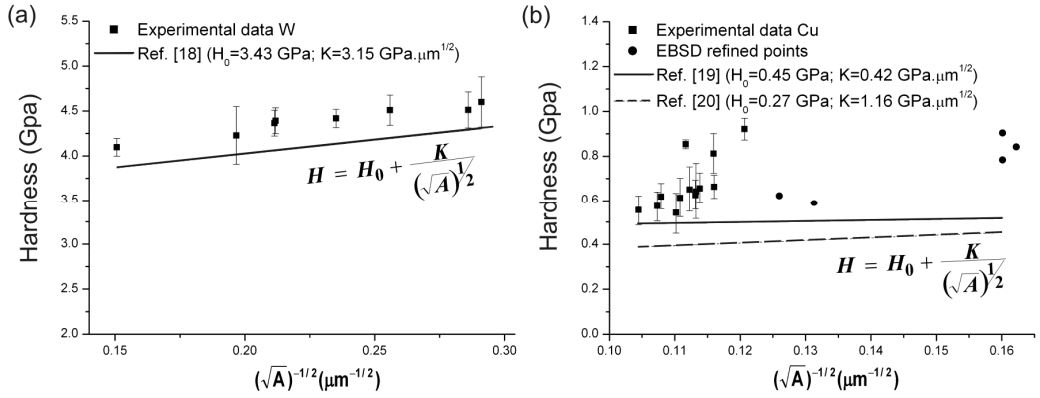

Figure 4. (a) Experimental relation between hardness and grain size (squares) and comparison with the literature (lines) for (a) W and (b) Cu. Grain size was refined by EBSD to take into account twins in Cu (circles), in this case hardness values were obtained by interpolation using a hardness vs distance curve.

Mitigation of hydrogen damage involves intervention at three levels:

(i) Hydrogen damage is strongly dependent on material factors (especially trap types, density and distribution) and suitable microstructural design is therefore an important mitigation approach. Microstructure refinement to the nanometer scale can suppress bubble formation or shift it to overall higher H lattice concentrations[13]. Furthermore, a nanostructure lessens radiation embrittlement due to an increased number of defect recombination sites.

(ii) Reduction of H permeation, which is controlled by implantation/adsorption rather than by diffusivity, can be achieved with residual compressive stresses [22] at the plasma facing surfaces. Surface barriers such as carbide films can also reduce H implantation/adsorption [13,23] and borides are likely to have the same effect. Surface modification treatments by implantation may be used for both purposes. Nevertheless, neutron irradiation may quickly reduce surface treatments effectiveness.

(iii) H_2 bubbles formation and coarsening are closely associated with grain growth. Therefore, strict temperature control both during working pulses and cleaning discharges is required. Partial desorption can be achieved with bakeout annealing [24]. Yet, this measure is constrained by microstructural coarsening and is greatly inefficient to remove recombined H in bubbles. Furthermore, the mitigation measures proposed in (i) can be expected to delay H desorption.

CONCLUSIONS

Severe H_2 bubble formation can occur in Langmuir probes exposed to the edge plasma during long-term regular operation of small fusion devices. The results suggest that this behavior should be monitored in larger reactors. Nucleation of high pressure bubbles at grain boundaries demonstrate that retention studies should consider microstructural characteristics such as grain size distribution and its evolution over time. Strategies for H damage mitigation have been discussed.

ACKNOWLEDGEMENTS

This work has been carried out within the Contract of Association between EURATOM and Instituto Superior Técnico. Financial support was also received from the Portuguese Science Foundation in the frame of the Associated Laboratory Contract.

REFERENCES

1. N. Baluc et al, Nucl. Fusion 47 (2007) S697
2. W.R. Wampler, B. LaBombard, B. Lipschultz, G.M. McCracken, D.A. Pappas, and C.S. Pitcher, J. Nucl. Mater. 266-269 (1999) 217
3. R. Andreani , M. Gasparotto, Fusion Eng. and Design 61/62 (2002) 27
4. R.A. Causey, T.J. Venhaus, Phys. Scripta T94 (2001) 9
5. D. Nunes, R. Mateus, I.D. Nogueira, P.A. Carvalho, J.B. Correia, N. Shohoji, R.B. Gomes, H. Fernandes, C. Silva, N. Franco, E. Alves, J. Nucl. Mater. (accepted for publication).
6. C. Jeynes, N.P. Barradas, P.K. Marriott, M. Jenkin, E. Wendler, G. Boudreault, R.P. Webb, J. Phys. D: Appl. Phys. 36 (2003) R97
7. Mayer, M., J. Likonen, et al., J. Nucl. Mater. 363-365 (2007) 101
8. M.J. Rubel, G.S. A. Kreter, A. Pospieszczyk, M. Psoda, P. Sundelin, E. Wessel, 34th EPS Conference on Plasma Phys. Warsaw, ECA. (2007) 31F
9. Y. Minyou, Plasma and Science & Tech. 7 (2005) 2828
10. R. Delamore, E. Ntsoenzok, F. Labohm, A. Van Veen, J. Grisolia, A. Claverie, Nucl. Inst. Met. B 186 (2002) 324
11. D. Nishijima, M. Y. Ye, N. Ohno, S. Takamura, 30th EPS Conference on Contr. Fusion and Plasma Phys., St. Petersburg, 7-11 July 2003 ECA Vol. 27A, P-2.163
12. S. H. Goods, J. Mater. Res. 6 (1991) 303
13. H. Wipf, Physica Scripta T94 (2001) 43
14. Hydrogen Damage and Embrittlement, ASM Handbook, 11 (2002)
15. S. Nakahara, Y. Okinaka, Ann. Rev. Mater. Sci. 21 (1991) 93
16. D.G. Ulmer, C. J. Altstetter, Acta Met. Matter. 39 (1991) 1237
17. P. Sofronis, Y. Liang, et al., Eur. J. Mech. - A/Solids 20 (2001) 857
18. Tungsten: Properties, Chemistry, Technology of the Element, Alloys and chemical compounds, Erik Lassner, Wolf-Dieter Schubert , 1999, Springer, 20
19. N. Hansen, B. Ralph, Acta Metall 30 (1982) 411
20. V.Y. Gertsman, M. Hoffmann, H. Leiter, R. Birringer, Acta Metall. Mater. 42 (1994) 3539
21. S. Nakahara, Y. Okinaka, Scripta Met. 19 (1985) 517
22. R.I. Kripyakevich, B. F. Kachmar et al. Mater. Sci. 6 (1973) 618
23. H. Atsumi, T. Tanabe, J. Nucl. Mater. 258-263 (1998) 896
24. S. O'Hira, A. Steinér et al. J. Nucl. Mater. 258-263 (1998) 990